



Noise Simulation Analysis of a Variable Displacement External Gear Pump and Unloading Groove Optimization

Yongkang Zhou, Wenwu Li, Dongpo Yang

College of Automotive Engineering, Shanghai University of Engineering Science, Shanghai, China
Email: yongkang_chou@126.com

How to cite this paper: Zhou, Y.K., Li, W.W. and Yang, D.P. (2018) Noise Simulation Analysis of a Variable Displacement External Gear Pump and Unloading Groove Optimization. *Open Access Library Journal*, 5: e5030.

<https://doi.org/10.4236/oalib.1105030>

Received: November 5, 2018

Accepted: November 24, 2018

Published: November 27, 2018

Copyright © 2018 by authors and Open Access Library Inc.

This work is licensed under the Creative Commons Attribution International License (CC BY 4.0).

<http://creativecommons.org/licenses/by/4.0/>



Open Access

Abstract

The oil pump is an important part of vehicle engine, whose noise and vibration characteristics affect the engine performance significantly. The noises generated by both the pressure and flow fluctuations are the main contributors to the oil pump noise. In this paper, noise analysis of an external gear pump is carried out by using the computational fluid dynamics (CFD) method and The Lighthill's acoustic analogy (LAA) algorithm. The fluid pressure and velocity distributions of the flowfield are firstly calculated by using a CFD model. The noises generated by flowfield are simulated and their sound pressure spectra are obtained by using an LAA-based finite element model. By analyzing the phenomenon of oil trapping, the optimum design of unloading groove is put forward, and then the simulation analysis is carried out. According to the finite element model, the noise level of gear pump is reduced and the effect of noise reduction is achieved. The technique presented in this paper can be regarded as a useful tool for optimization design of gear pumps in vehicle engineering.

Subject Areas

Automata, Mechanical Engineering

Keywords

Gear Pump, Noise Calculation, Unloading Groove

1. Introduction

It is well known in the vehicle engineering that there is a continuous demand for the component manufacturers to reduce noise and vibration levels of their

products, due to the reason of vehicle ride comfort [1]. The external gear pump is a simple and robust device that can work at a wide range of pressure and rotational speeds. These features make them widely accepted as lubrication pumps in machine tools, oil pumps in engines or in fluid power transfer units in the aerospace, power generation, agricultural and automotive industries. However, the main drawbacks of the external gear pump are related to high noise and vibration levels [2] [3]. Generally, the external gear pumps are often accompanied with noise levels that are higher than other types of pumps.

In a gear pump, the meshing of gears is used to pump fluid. There are two main sources of vibration and noise, sharing the same fundamental frequencies [4]. One is the periodic variation of the pressure distribution on the gears, due to the fluid flows from the low to the high pressure chamber. The other is the periodic variation of gear meshing force [5] [6]. It has been found that the fluid-borne noises are the main contributors to the noise level of an external gear pump, which needs further research in engineering.

In this present work, the noise of a variable displacement external gear pump used in vehicle engine is studied. The CFD model is used to estimate the pressure and velocity distributions around the gears. The LAA is used to simulate the fluid-borne noises. The noise distributions and characteristics under some typical operating conditions of the pump are obtained. The work conducted in this paper is instructive to engineers for fluid-sound analysis and design of the gear pump structures.

2. Structure of a Variable Displacement External Gear Pump

The gear pump studied in this paper is a variable displacement gear pump, which is an electrical controlled self-adjustable pump with advantages of more accurate in control, more efficient in operation and high fuel economy of the engine. This pump can accomplish the transformation between low and high pressures by an electromagnetic valve that controlled by the engine electronic control unit (ECU).

The structure exploded view of the sample gearpump is shown in **Figure 1**.

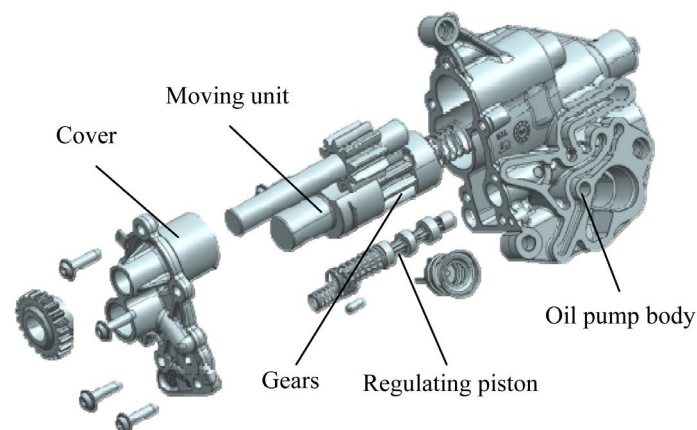


Figure 1. An exploded view of a variable displacement external gear pump.

3. Noise Calculation

3.1. CFD Modeling and Calculation in Flow Field

Physical model of the gear pump is established in CAD software. A three-dimensional flow field model of the pump can be obtained through the Boolean calculations such as union, intersection, and subtraction. The meshing of flow field model is completed in the Pump Linx software [7]. The automatic mesh generator based on geometry conformal adaptive binary-tree algorithm is applied.

The finite volume method with collocated grids is used to solve the 3-D transient viscous fluid mechanics equation in this paper. The SIMPLEC method [8], which has been proved suitable for low speed fluids, is adopted in the CFD calculation. The accurate dynamic mesh method is utilized to treat the pump movement. The moving and static flow channels are modeled respectively. During calculations, the moving flow channel can process the grids' movement and deformation automatically. In each time step, the moving and static fields will be automatically linked in a new position through the fully implicit gliding interface technology. The gear position in the variable displacement pump at different rotational speeds can be determined by Equation (1).

$$B = q / (AZm^2n) \quad (1)$$

where B is the meshing length of the gears, q is the fluidflow, Z is the gear teeth number, m is the gear module, n is the rotational speed and A is a correction factor equals to 5.3 in this paper [14]. Using Equation (1), one may easily calculate that the gear pump is at the state of half-meshing at 3000 rpm and 5000 rpm.

3.2. Lighthill's Acoustic Analogy Method

In this paper, the FE model is established based on the LAA algorithm and the Curle's theory under the following assumptions: 1) the body source in the FE region is from the volume integral of Curle's equation; 2) the boundary conditions are from the surface integral of Curle's equation and 3) other boundary condition is from green function of free field.

The LAA equations [9] can be written as:

$$\frac{\partial^2 \rho_a}{\partial t^2} - a_0^2 \frac{\partial^2 \rho_a}{\partial x_i \partial x_i} = \frac{\partial^2 T_{ij}}{\partial x_i \partial x_j} \quad (2)$$

$$T_{ij} = \rho v_i v_j + \delta_{ij} \left((p - p_0) - a_0^2 (\rho - \rho_0) \right) - \tau_{ij} \quad (3)$$

where $\rho_a = \rho - \rho_0$ is the sound pressure, ρ and p are the local density and pressure of the fluid in a flow field; ρ_0 and p_0 are the reference density and pressure, respectively, and a_0 is the sound speed. τ_{ij} is the viscous stress tensor, v_i and v_j are the flow field component in the i and j directions, respectively.

Defining $\rho_a = -i\omega\phi/a_0^2$ the corresponding acoustic analogy frequency equation is defined by:

$$\frac{\omega^2}{a_0^2} \varphi + \frac{\partial^2 \varphi}{\partial x_i \partial x_i} = \frac{1}{i\omega} \frac{\partial^2 T_{ij}}{\partial x_i \partial x_j} \tag{4}$$

After finite element integration of the LAA equation [10] [11] and rearrangement, one can obtain a discrete weak solution in the form of finite-element variational,

$$\iiint_{\Omega} \left(\frac{\partial^2 \rho_a}{\partial t^2} \delta \rho_a + a_0^2 \frac{\partial \rho_a}{\partial x_i} \frac{\partial (\delta \rho_a)}{\partial x_i} \right) dx dy dz = S \tag{5}$$

where the source S on the right includes both the body and surface sound sources. The sound sources can be directly solved from the current numerical model as follows. As mentioned above, after the scalar function φ is defined, the corresponding finite element weak form infrequency is:

$$-\iiint_{\Omega} \frac{\omega^2}{\rho_0 a_0^2} \varphi \delta \varphi dx dy dz - \iiint_{\Omega} \frac{1}{\rho_0} \frac{\partial \varphi}{\partial x_i} \frac{\partial (\delta \varphi)}{\partial x_i} dx dy dz = s_{\Omega} + s_{\Gamma} \tag{6}$$

The body sound source is:

$$s_{\Omega} = \iiint_{\Omega} \frac{i}{\rho_0 \omega} \frac{\partial (\delta \varphi)}{\partial x_i} \frac{\partial T_{ij}}{\partial x_j} dx dy dz \tag{7}$$

The surface sound source, on the boundary of computational domain, is:

$$s_{\Gamma} = -\iint_{\Gamma} \frac{1}{\rho_0} F(\Sigma_{ij}) d\Gamma(\vec{x}) \tag{8}$$

The sound source item in the time domain can be provided by the CFD velocity field. After Fourier transform, the sound source term in frequency domain $T_{ij}(\vec{x}, \omega) \approx \rho v_i v_j$ is obtained, thereby the sound source. After the FE discrete equation is solved in frequency domain, the LAA analysis of a sound field is finished.

3.3. Noise Calculation and Validation

Considering the requirements in acoustical computation, there should be at least 6 elements within the shortest wavelength of the sound [12]. The tetrahedral solid elements are selected in this paper. To analyze the radiation characteristics, a sound propagation region is added when calculating the sound propagation of the sound source. A layer of infinite element in outer most border is set as a boundary condition of the sounds without reflections. The half of the established FE model of the gear pump is shown in **Figure 2**.

The grid of the gear pump meshing area is created at the position of addendum circle. The fluid area grid of the pump is also set up (**Figure 3**). Two important components: the Lighthill surface and volume are setup in the Actran software. In Actran, the flow field information can be transformed into sound source information by the ICFD module. Performing the ICFD in the Actran, the flow field information previously calculated by the Pump Linx software, such as the pressure, velocity and density of the fluid, is interpolated into the Lighthill surface and volume and set as the acoustical excitation sources. The FE calculated

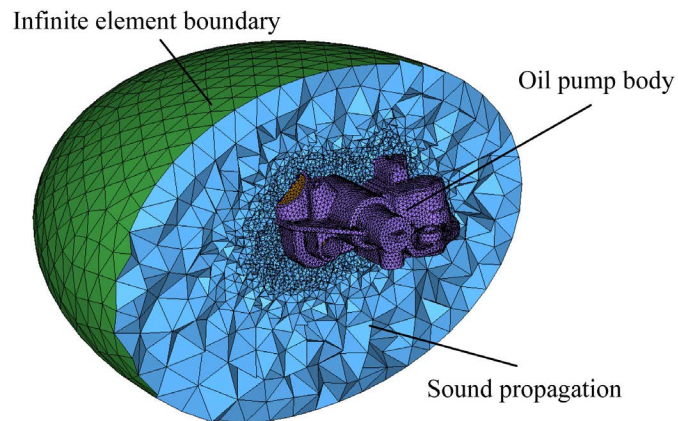


Figure 2. The established finite element model of the gear pump.

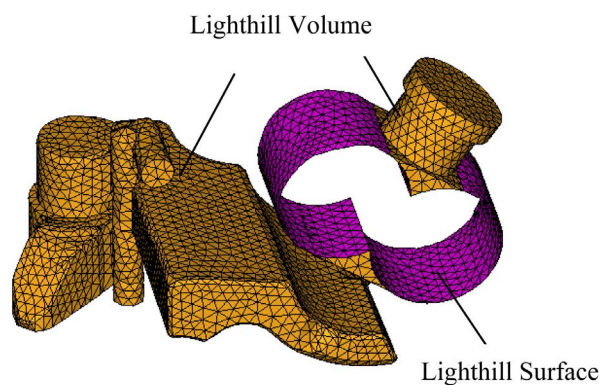


Figure 3. The grid of the acoustic source: Lighthill volume and Lighthill surface.

results calculated in the Actran are in time domain. Using the Fourier transform, the excitation sources can be transferred into the frequency domain. The frequency responses can be directly obtained by setting a frequency range from 20 to 4000 Hz in the Actran.

The A-weighted sound pressure level (SPL) calculated by the Actran at low pressure 1.8 bar, 1000 rpm and 3000 rpm, and high pressure 3.3 bar, 5000 rpm, are shown in **Figure 4**.

When the shaft rotational speed of the gear pump is at a low level, the pulsations of pressure and flow caused by the shaft rotation are not obvious, and the peak values of the harmonics are small. The harmonic phenomena are mainly caused by gear meshing. As shown in **Figure 4**, the first four primary harmonics of 3000 rpm appeared sequentially at 80 Hz, 170 Hz, 500 Hz and 1000 Hz.

As the rotational speed increases, the pressure and flow pulsation induced by the rotating shaft increases. At the speed of 5000 rpm, except for the primary harmonics, many secondary harmonics appear at 50, 100, and 150 Hz, etc. When the rotational speed reaches 5000 rpm, at the scale from 250 Hz to 800 Hz and 1500 Hz to 2500 Hz, there are a lot more harmonics in **Figure 4** than at 3000 rpm. When the rotational speed reaches 5000 rpm, the secondary harmonics are mainly caused by the rotating shaft, which is shown in **Figure 4**.

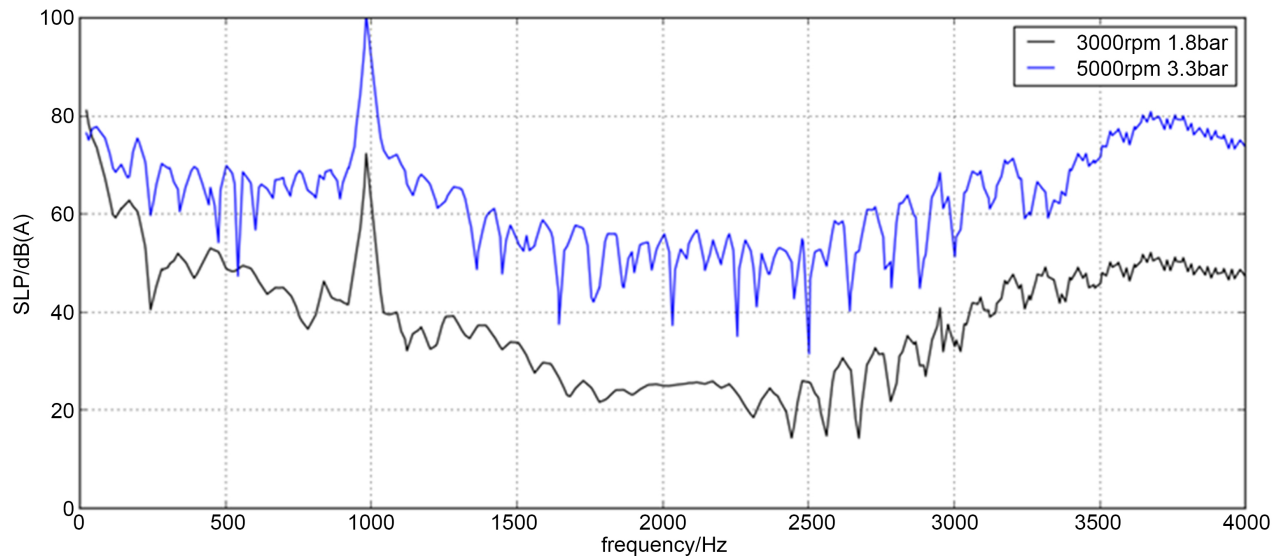


Figure 4. Simulated results of the A-weighted sound pressure levels at 3000 rpm (1.8 bar) and 5000 rpm (3.3 bar).

4. Optimization of Unloading Groove

4.1. Design of Unloading Groove

To design the unloading groove of gear pump, it is necessary to ensure that, at any time, there must be a meshing point in the sealing belt between the two unloading grooves. Because only in this way, it will not lead to gear pump suction cavity. The following two conditions must be satisfied:

- 1) Two the sealing belt between the unloading grooves should cover the whole single tooth meshing area.
- 2) The distance between the two unloading grooves shall not be less than the projection of the length of the normal pitch of a gear on the meshing line on the normal direction of the connecting line of the two gears. That is the distance between the two unloading grooves.

On the below figure, the solid line is the center line of the two gears, and the dashed line is the limit position of the unloading groove. The specific position of the unloading groove is shown in **Figure 5**.

The effective method to reduce the pressure fluctuation in the oil trapped area is to open the unloading groove. Based on the existing unloading groove of the pump, combined with its working principle, the method is put forward to open the unloading groove at the moving unit of the driven shaft (side of the upper end of the piston). When the rotational speed of the pump increases, the driven shaft drives the driven gear downward, the meshing width of the gear decreases, and the pressure fluctuation of the oil trapped area increases.

The shape of unloading groove in this paper is trapezoidal groove (Groove 1), trapezoidal groove and diversion groove (Groove 2), as shown in **Figure 6**. As the moving unit moves down, the unloading space of the unloading tank gradually increases, which can better reduce the pressure fluctuation of the oil trapped area at high pump speed.



Figure 5. Specific location of unloading groove.

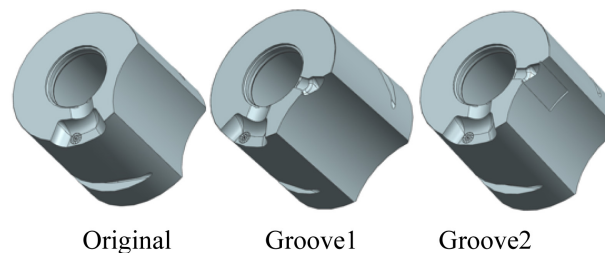


Figure 6. The shape of unloading groove.

4.2. Noise Calculation and Validation

Figure 7 is the simulation SPL curve of the original pump, unloading groove pump and unloading groove and diversion groove pump under the rotational speed reaches 3000 rpm. As can be seen from the graph, in addition to individual frequencies, the SPL of the unloading groove pump and unloading groove and diversion groove pump is lower than that of the original pump. This indicates that the two schemes can effectively reduce noise.

Overall, the sound pressure level of unloading groove and diversion groove pump is better than that of unloading groove pump. When the frequency is between 0 Hz and 1500 Hz, the sound pressure level of unloading groove and diversion groove pump is lower than that of unloading groove pump. When the frequency is between 1500 Hz and 2500 Hz, the sound pressure level of unloading groove pump is lower than that of unloading groove and diversion groove pump. Finally, when the frequency is between 2500 Hz and 4000 Hz, the sound pressure level of unloading groove and diversion groove pump is lower than that of unloading groove pump.

Figure 8 is the simulation SPL curve of the three types of pumps under the rotational speed reaches 5000 rpm.

The sound pressure level of the unloading groove pump and unloading groove and diversion groove pump at 5000 rpm is not as good as that at 3000 rpm. However, in most frequency bands, the noise level of the unloading groove pump and unloading groove and diversion groove pump is lower than that of the original pump. Obviously, the sound pressure level of the unloading groove

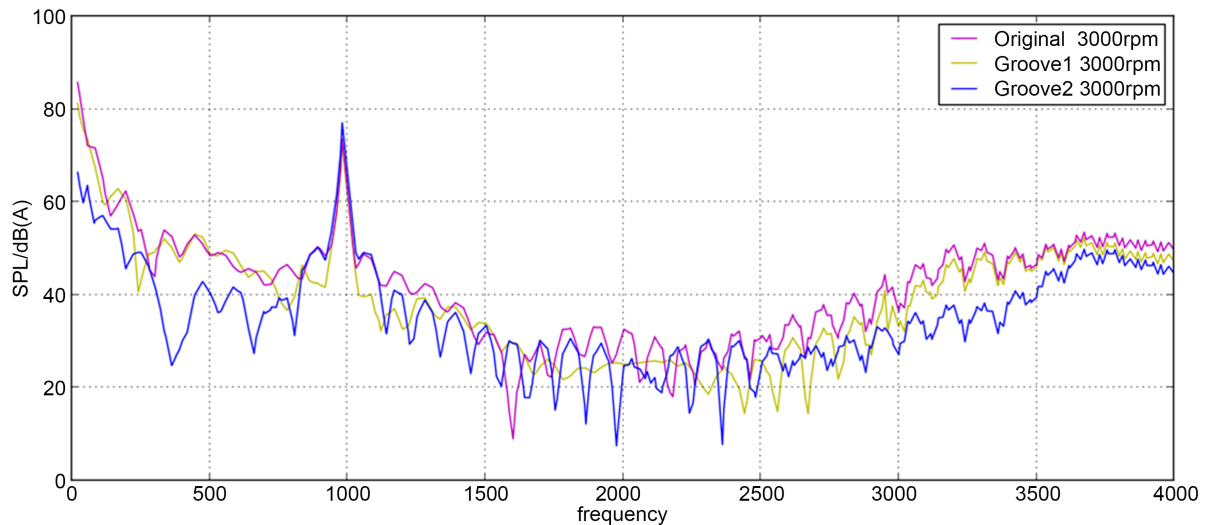


Figure 7. Sound pressure spectra: simulation results of original pump, unloading groove pump and unloading groove and diversion groove pump at 3000 rpm.

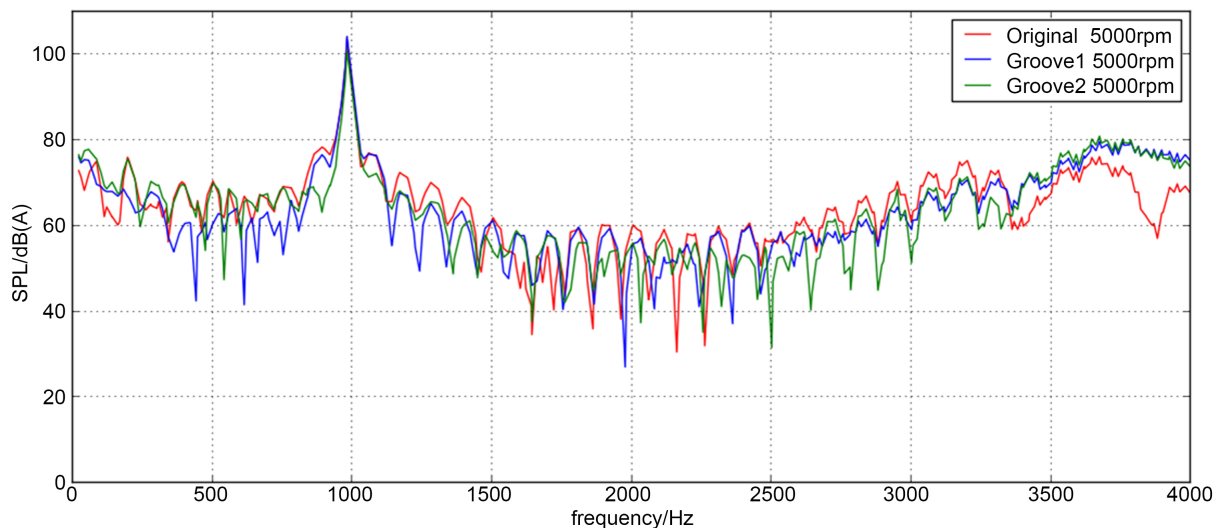


Figure 8. Sound pressure spectra: simulation results of original pump, unloading groove pump and unloading groove and diversion groove pump at 5000 rpm.

pump almost below the whole frequency band is lower than that of the original pump except 3400 Hz to 4000 Hz band.

5. Conclusion

A model for noise analysis of a variable displacement external gear pump is established. A FE combined numerical model for fluid noise simulation of the gear pump is established based on the Lighthill acoustic analogy algorithm. The sound energy distributions of the gear pump are obtained by frequency response analysis in the Actran. The newly established model can be used to estimate the noise characteristics of variable displacement external gear pumps. Engineers can do simulating analysis for existing products or products in development using

this method in order to verify whether the noise level of products meets the relevant standards.

The result of simulation analysis shows that the two newly designed unloading grooves have the effect of reducing the fluid noise of gear pump obviously. The noise reduction effect of unloading groove is better than that of original and unloading groove and diversion groove, when the rotational speed is 3000 rpm and 5000 rpm. Therefore, unloading groove is selected as the noise reduction scheme. Furthermore, by changing the structure of the oil pump model, one can reduce the noise level and shorten the product development expenses and time as well. This is instructive and meaningful for fluid noise calculations in engineering.

Conflicts of Interest

The authors declare no conflicts of interest regarding the publication of this paper.

References

- [1] Mucchi, E., Dalpiaz, G. and Fernandez, A. (2012) Elasto-Dynamic Analysis of a Gear Pump. Part I: Pressure Distribution and Gear Eccentricity. *Mechanical Systems and Signal Processing*, **24**, 2160-2179. <https://doi.org/10.1016/j.ymssp.2010.02.003>
- [2] Nagakura, H. and Kojima, E. (1982) Characteristic of Fluidborne Noise Generated by Fluid Power Pump: 1st Report, Mechanism of Generation of Pressure Pulsation in Axial Piston Pump. *Bulletin of JSME*, **25**, 46-53. <https://doi.org/10.1299/jsme1958.25.46>
- [3] Yoshino, T., Kojima, E. and Shinada, M. (1982) Characteristic Offfluid-Borne Noise Generated by Fluid Power Pump: 2nd Report, Pressure Pulsation in Balanced Vane Pump. *Bulletin of JSME*, **27**, 475-482.
- [4] Dunlop, R.W. (1984) Vibration and Noise Characteristics of Positived Is Placement Pumps. *InterNoise*, **84**, 127-131.
- [5] Mucchi, E., Dalpiaz, G. and Rivola, A. (2010) Elastodynamic Analysis of a Gear Pump. Part I: Pressure Distribution and Gear Eccentricity. *Mechanical Systems and Signal Processing*, **24**, 2180-2197. <https://doi.org/10.1016/j.ymssp.2010.02.004>
- [6] Li, Y.Z., Gao, L.H. and Tang, X.Y. (2011) The Flow Pulsation Analysis of External Gear Pump. *Advanced Materials Research*, **236**, 2327-2333. <https://doi.org/10.4028/www.scientific.net/AMR.236-238.2327>
- [7] Frosina, E., Senatore, A. and Buono, D. (2014) A Tridimensional CFD Analysis of the Oil Pump of an High Performance Motorbike Engine. *Energy Procedia*, **45**, 938-948. <https://doi.org/10.1016/j.egypro.2014.01.099>
- [8] Gao, Q., Wu, W.W. and Li, J.G. (2011) Fluid Characteristics Analysis of Cycloid Rotor Oil Pump. *Machine Tool & Hydraulics*, **39**, 29-33.
- [9] Lighthill, M.J. (1952) On Sound Generated Aerodynamically I. Generaltheory. *Proceedings of the Royal Society of London A*, **211**, 564-587. <https://doi.org/10.1098/rspa.1952.0060>
- [10] Caro, S., Ploumhans, P. and Gallez, X. (2004) Implementation of Lighthill's Acoustics Analogy in a Finite/Infinite Elements Framework. *10th AIAA/CEAS Aeroacoustics Conference*, Manchester, 10-12 May 2004.

- [11] Caro, S., Ploumhans, P. and Gallez, X. (2005) Identification of the Appropriate Parameters for Accurate CAA. *11th AIAA/CEAS Aeroacoustics Conference*, Monterey, 23-25 May 2005. <https://doi.org/10.2514/6.2005-2991>
- [12] Wang, Z.G. (2007) *The Theory of Acoustic Finite Element Analysis and Engineering Application*. National Defense Industry Press, Beijing.